J Mater Sci (2010) 45:3397–3404
DOI 10.1007/s10853-010-4346-2

Synthesis and properties of ceramic fibers from polycarbosilane/polymethylphenylsiloxane polymer blends

Ken'ichiro Kita · Masaki Narisawa · Atsushi Nakahira · Hiroshi Mabuchi · Masaki Sugimoto · Masahito Yoshikawa

Received: 16 November 2009 / Accepted: 22 February 2010 / Published online: 17 April 2010

Abstract We synthesized ceramic fibers based on silicon carbide (SiC) from polymer blends of polycarbosilane (PCS) and polymethylphenylsiloxane (PMPhS) by melt-spinning and radiation curing. PMPhS was compatible with PCS up to 30 mass%, and formed a transparent melt at temperatures higher than 513 K. The softening point was also lowered by adding PMPhS and 15 mass% of PMPhS to PCS was the most suitable condition for obtaining thin fibers with an average diameter of 14.4 μm. Due to the lowered softening point of the PCS–PMPhS fibers, γ-ray curing in air was adopted. The ceramic yield of the cured fiber was 85.5% after pyrolysis at 1273 K. In spite of the small diameter, the resulting tensile strength at 1273 K was rather limited at 0.78 GPa. Blooming of the PMPhS component during pyrolysis may have caused surface defects. After high-temperature pyrolysis at 1673–1773 K, a porous nanocrystalline SiC fiber with a unique microstructure was obtained with surface area of 70–150 m^2/g. When the fiber was pyrolyzed at the same temperature under a highly reductive atmosphere, wire bundle-shaped fibers were obtained by gas evolution and reactions.

Introduction

In 1970s, Yajima et al. invented a method for producing silicon carbide (SiC) fiber from polycarbosilane (PCS) through melt-spinning, curing, and pyrolysis [1–3]. This method is called the "precursor method." After this invention, many experiments have been attempted to improve ceramic fibers. In recent years, various advanced SiC fibers based on such technological advances have been widely commercialized and used as reinforcements for ceramic matrix composites (Hi-Nicalon [Nippon Carbon Co., Ltd.], Tyranno SA [Ube Industry Co., Ltd.]) [4, 5].

The study of polymer blends containing PCS and other organometallic polymers showed that some organometallic polymers improve the melt-spinnability of a polymer blend. For example, a combination of PCS and polyvinylsilane (PVS) was effective for synthesizing thin flexible fibers [6, 7]. Such applications of polymer blend techniques in conjunction with the precursor method are helpful for developing new precursors at rather low cost by adjusting combinations.

We have focused on polymethylphenylsiloxane (PMPhS), which includes phenyl groups with a siloxane main chain structure. It is thought that the—π-π-interaction among phenyl groups is expected to improve the melt-spinnability of the polymer blends. Moreover, it has been reported that PMPhS develops in liquid crystals according to a certain thermal history [8, 9]. Liquid crystal formation has been utilized in the field of pitch-based carbon fibers, and also shows promise for achieving high intermolecular interactions and improved melt-spinnability [10]. In addition, the reaction of free carbon originating from the phenyl groups with SiOC coordination originating from the siloxane main chain at high temperatures yield a SiC nanocrystalline structure incorporated in amorphous Si–C.

In this study, we investigated the characteristics of a PCS-based precursor modified with PMPhS for synthesizing SiC-based fibers, in particular, after high-temperature pyrolysis.

K. Kita (✉) · M. Narisawa · A. Nakahira · H. Mabuchi
Graduate School of Engineering, Osaka Prefecture University, Sakai, Osaka 599-8531, Japan
e-mail: hz302@mtr.osakafu-u.ac.jp

M. Sugimoto · M. Yoshikawa
Quantum Beam Science Directorate, Japan Atomic Energy Agency, Takasaki, Gunma 370-1292, Japan

Experimental procedure

Commercialized PMPhS (KF-54, Shin-etsu Chemicals Co., Ltd., Tokyo, Japan) was blended with PCS (NIPUSI-Type A, Nippon Carbon Co., Ltd., Tokyo, Japan). The blend ratios of PMPhS to PCS were 3, 15, and 30 mass% for the purpose of comparison. Polymer blend solutions in benzene were freeze-dried to obtain white powders. The prepared polymer blends containing 3, 15, and 30 mass% of PMPhS were identified as PS03, PS15, and PS30.

Viscosities of polymer blends were measured with a viscometer (RB-80R, Toki Sangyo Co., Ltd., Tokyo, Japan) in N_2 atmosphere. Thermogravimetric analysis of PS15 at 473–553 K was performed with an electronic balance (BP310P, Sartorius K.K., Göttingen, Germany) and electric furnace (ARF-50M, Asahi-Rika Corporation, Chiba, Japan) in an Ar flow. In this analysis, the heating rate was set at 10 K/h between 473 and 553 K. IR spectra for PS15 heated at 573 K were obtained using an FT-IR Spectrometer (Spectrum GX, Perkin Elmer Japan Co., Ltd., Yokohama, Japan).

These polymer blends were melt-spun at 523–533 K into preceramic fibers, which were observed using an optical microscope (VH-Z450, KEYENCE Corporation, Osaka, Japan). The fibers were cured by γ-ray irradiation in air or electron beam irradiation in He atmosphere. In γ-ray curing, the dose rate was fixed at 6.45×10^2 C/kg h and the fibers were irradiated for 96 h. In electron beam curing, the first dose rate was 0.4 kGy/s and the fibers were irradiated for 1000 s. The second dose was administered 2000 s after the first irradiation, at a rate of 0.79 kGy/s, while the final dose was administered 4000 s after the second irradiation at a rate was 1.58 kGy/s. The fibers were heated at 773 K in order to prevent fiber oxidation due to the influence of residual radicals [11]. After curing, the fibers were pyrolized at 1273 K for 1 h in inert atmosphere, and the pyrolized fibers were re-pyrolyzed at 1573–1773 K for 30 min in Ar flow. In addition, we sought to re-pyrolyze PS30 fibers at 1773 K by the same apparatus with diminished Ar flow (5 mL/min). During pyrolysis and re-pyrolysis, the heating rate was set at 200 K/h.

The pyrolyzed and the re-pyrolyzed fibers were also observed with an FE-SEM (JSM-6700F, JEOL Ltd., Akishima, Japan). X-ray diffraction patterns of these fibers were obtained using an X-ray diffractometer (GeigerFlex Rad and CN2182D5, Rigaku Corporation, Akishima, Japan). The tensile strength of these fibers was measured at room temperature using a tensile testing machine (Model-1305D, AIKOH ENGINEERING Co., Ltd., Higashiosaka, Japan) with a gauge length of 10 mm and a crosshead speed of 2 mm/min. The average tensile strength was obtained from the measured results of more than 20 filaments. The surface areas of these fibers were measured by the BET method with an automatic surface area analyzer (Macsorb HM model-1201, Mountech Co., Ltd., Tokyo, Japan).

Result and discussion

Effect of PMPhS addition on fiber melt-spinning and fiber pyrolysis

Figure 1 shows that the relationship between viscosity and temperature for PCS, PS03, PS15, and PS30. The softening points of PCS, PS03, PS15, and PS30 were 593, 583, 543, and 513 K, respectively, and 30 mass% is the limit for PMPhS compatibility. Beyond this, the melt showed a turbid appearance. In particular, the viscosity of PS15, a composition most suitable for melt-spinning, showed moderate temperature dependence. The appropriate viscosity of a polymer melt for fiber-spinning in our apparatus was 5–20 Pa s [6]. From a practical viewpoint, this means that PS15 can accommodate wide temperature fluctuations during melt-spinning. From a scientific viewpoint, such moderate temperature dependence corresponds to low activation energy of viscous flow and weak interactions between macromolecules in the polymer melt. In PCS and PS03, the interaction between PCS molecules was dominant, while that between PMPhS molecules was dominant in PS30. PS15 is probably positioned at an intermediate state. Such a plasticizer effect of additional polymer to PCS has been observed in cases of polyvinylsilane (PVS) and polymethylhydrosilane (PMHS) [6, 12]. However, the addition of PMPhS showed a marked effect in contrast to previous cases, even at a low content.

Figure 2 shows the optical micrographs of PS15 and PS30 fibers after melt-spinning with transmitted light.

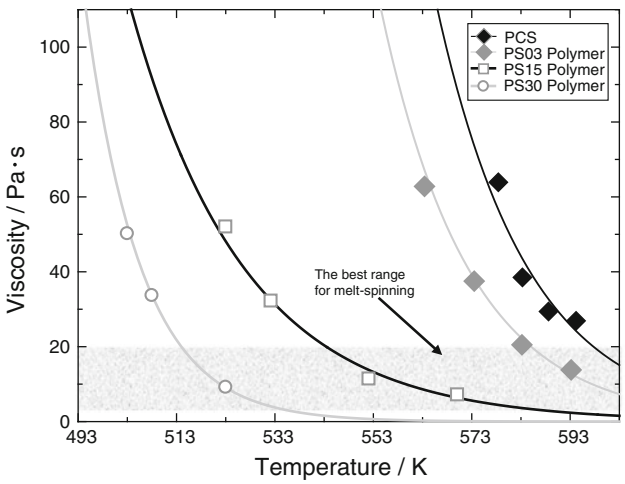

Fig. 1 The relationship between melt viscosity and temperature of PCS and PCS–PMPhS polymer blend in N_2 atmosphere

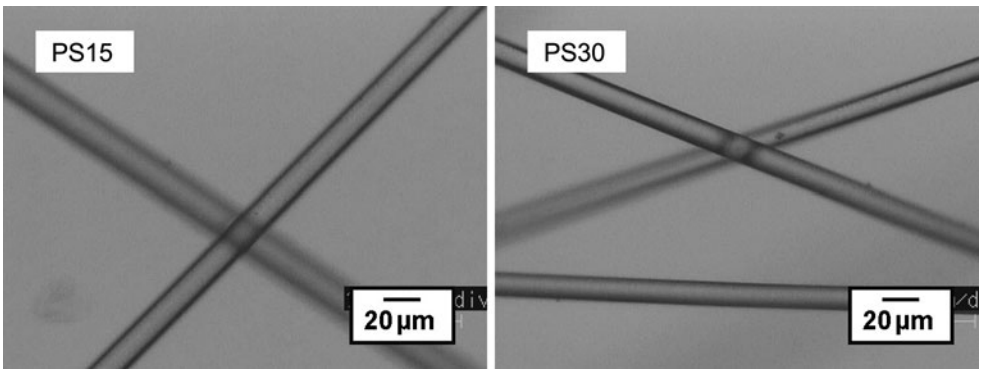

Fig. 2 The optical micrographs of PS15 and PS30 fibers after melt-spinning with transmitted light

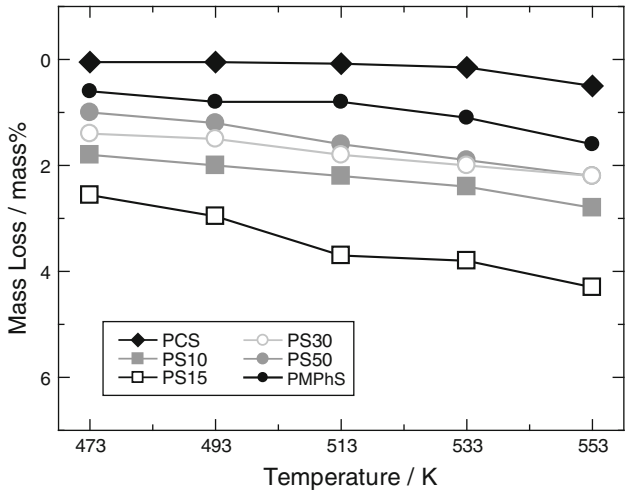

Fig. 3 The mass loss of the various polymer blends after heat treatment from 473 to 553 K

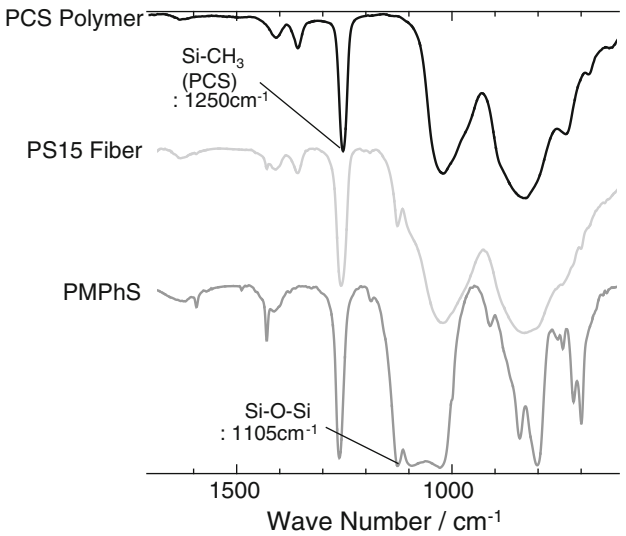

Fig. 4 The IR spectra of PCS, PS15 fibers melt-spun at 553 K and PMPhS

These fibers were completely transparent, a result consistent with the observed transparency and viscosity of blend polymer melts.

Since melt-spinning is carried out at 523–533 K, polymer decomposition must be taken into account. In order to estimate the degree of polymer decomposition, we investigated mass loss after heat treatment at 473–553 K, the results of which are shown in Fig. 3. PS10-50, however, showed a mass loss of 1–3% at 533 K. This value is relatively small and acceptable for melt-spinning. IR spectra also revealed that the composition of the precursor fiber is maintained after melt-spinning. Interestingly, the heat stability of the polymer blends was reduced relative to that of pure PCS or of pure PMPhS. The weakened interaction between macromolecules, which has been suggested from viscosity measurements, may permit volatilization of low-molecular weight components in PS10-50 at rather low temperatures.

Figure 4 shows FT-IR spectra for PCS, PS15 polymer blend, PS15 fibers melt-spun at 553 K, and PMPhS. The

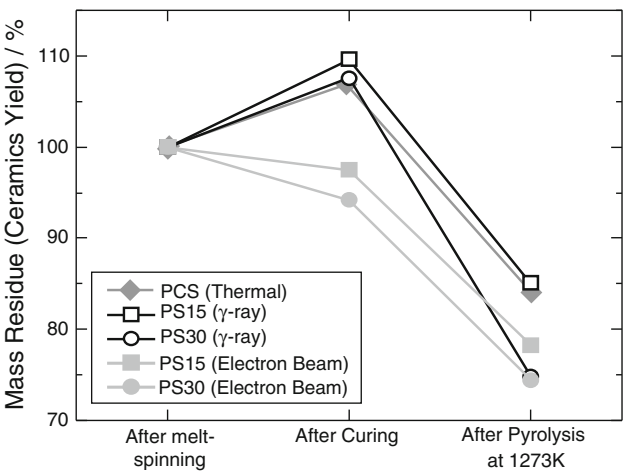

Fig. 5 The rate of mass residue of PCS, PS15, and PS30 fibers after melt-spinning, curing, and pyrolysis at 1273 K

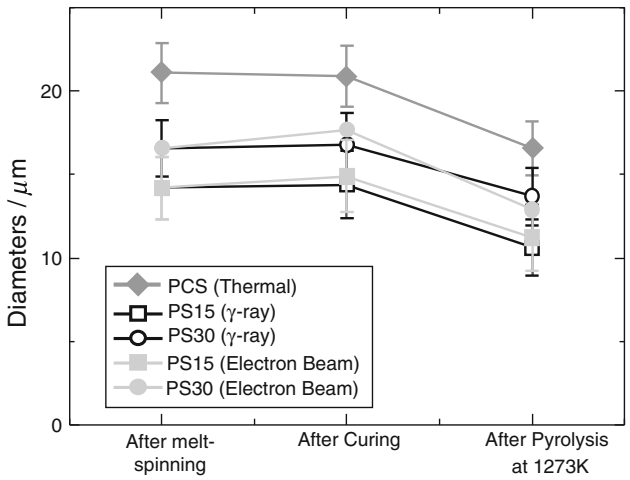

Fig. 6 The diameters of PCS, PS15, and PS30 fibers of after melt-spinning, curing, and pyrolysis at 1273 K

Table 1 The tensile strengths of PCS, PS15, and PS30 cured by γ-ray or electron beam after pyrolysis at 1273 K cured by γ-ray or electron beam

Samples	Tensile strength (GPa)
PCS (Thermal)	1.86
PS15 (γ-ray)	0.64
PS30 (γ-ray)	0.29
PS15 (Electron beam)	0.74
PS30 (Electron beam)	0.36

absorption band of Si–CH_3 (1250 cm^{-1}) was adopted as a standard for spectral normalization. PMPhS appeared to remain in the as-spun fiber state because the Si–O–Si absorption band (1105 cm^{-1}), which in not included in PCS, was evident in the fiber.

Figure 5 shows the mass residue of PCS, PS15, and PS30 fibers after melt-spinning, curing and pyrolysis at 1273 K. The mass of the fibers after melt-spinning was used as the standard. After the thermal curing process, the fiber was melted during heating. The softening point of PCS–PMPhS may be too low to permit thermal curing. The mass gains of PS15 and PS30 fibers cured by γ-ray oxidation were 9.67% and 7.61%, respectively, and the ceramic residues of PS15 and PS30 fibers after pyrolysis at 1273 K were 85.1% and 74.8%, respectively. As for electron beam nonoxidation curing, the mass losses of PS15 and PS30 fibers after curing and successive annealing processes were 3.50% and 5.92%, respectively. The ceramic residues of PS15 and PS30 fibers after pyrolysis at 1273 K were 78.2% and 74.4%, respectively. In PS30 cured by γ-ray oxidation, the ceramic residue was low relative to PS15, although the spun fibers captured a sufficient amount of oxygen. Decomposition of phenyl groups in PMPhS may be accelerated by the captured oxygen [13].

Figure 6 shows the diameters of PCS, PS15, and PS30 fibers after melt-spinning, curing, and pyrolysis at 1273 K. The average diameters of PCS, PS15, and PS30 fibers, respectively, after melt-spinning were 21.1, 14.4, and

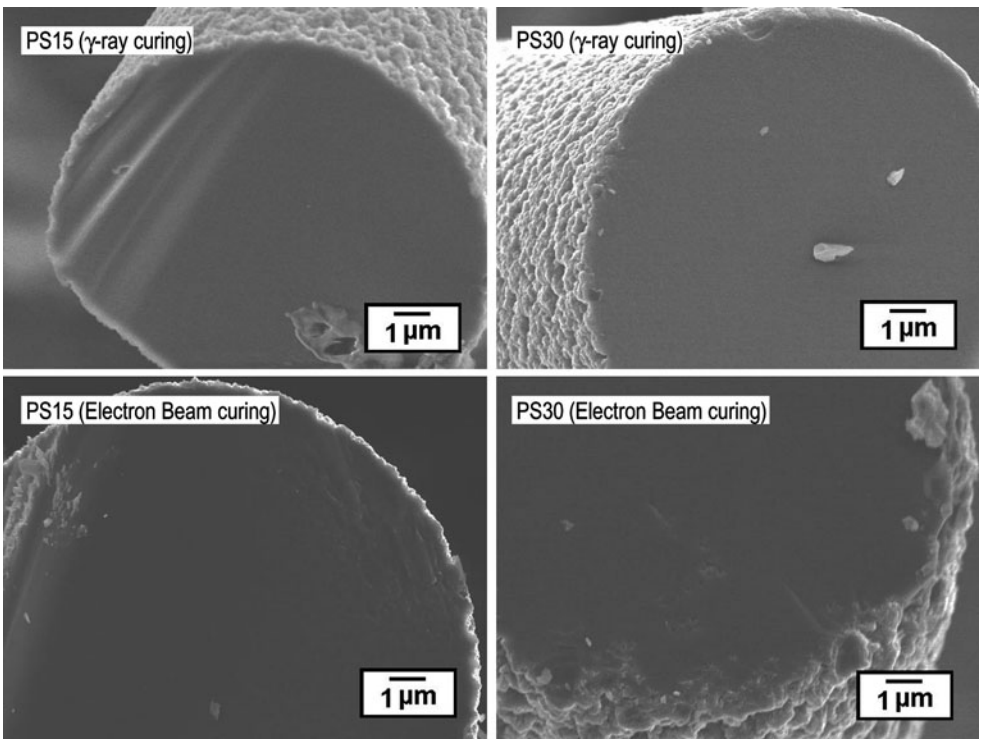

Fig. 7 The FE-SEM images of the cross sections of PS15 and 30 fibers pyrolyzed at 1273 K in 1 h under inert atmosphere

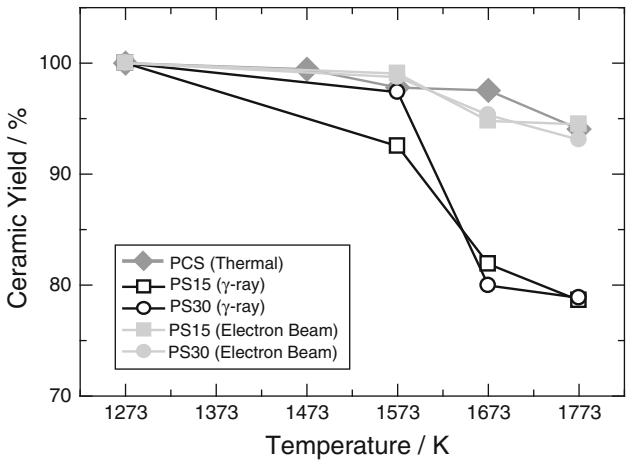

Fig. 8 The residual mass of PCS, PS15, and PS30 fibers after re-pyrolysis beyond 1273 K

16.6 μm. This suggests strongly that PMPhS acts as a plasticizer and that the fine fibers are obtained by the improved melt-spinnability.

It is known that the tensile strength of brittle fibers increases with decreasing diameter due to decreased surface defects per length. However, the strengths of PS 15 and 30 did not exceed 1 GPa. Table 1 shows the tensile strength of the fibers after pyrolysis at 1273 K. The tensile strength of PCS fibers was 1.86 GPa. In the case of PS15 fibers, the strengths of those cured by γ-ray and electron beam, respectively, were 0.64 and 0.74 GPa. As for PS30 fibers, the strengths of those cured by γ-ray and electron beam, respectively, were 0.29 and 0.36 GPa. Compared with expectations, the strengths of PS15 and PS30 fibers were relatively low.

Figure 7 shows SEM images of PS15 and 30 fibers. The inner area of the cross section is smooth, whereas the surface of the fiber is quite rough. Moreover, images of PS30 fibers showed some cracks in the surface of the fiber. This reveals that PMPhS in the polymer blend can easily cause thermal decomposition. In turn, this decomposition is thought to cause the decrease in tensile strength.

Microstructures in the fiber after re-pyrolysis at 1773 K

Figure 8 shows the residual masses of PCS fiber, PS15 fibers, and PS30 fibers after re-pyrolysis beyond 1273 K. The mass of the fibers after pyrolysis at 1273 K was used as the standard. The masses of PS15 and PS30 fibers cured by γ-ray oxidation decreased rapidly between 1573 and 1673 K, and the mass losses were about 22% up to 1773 K. On the other hand, mass losses for the other fibers were around 5% up to 1773 K. It is well-known that CO–SiO gas is actively evolved from cured Si–C–O polymer in the same temperature range [13, 14]. The decomposition of Si–C–O in PS fibers with γ-ray curing may be accelerated by incorporating a siloxane-based structure or by increasing nucleation sites.

Figure 9 shows the FE-SEM images of PS15 fibers re-pyrolized at 1773 K for 0.5 h under an inert atmosphere. The cross section of PS15 fiber cured by γ-ray oxidation is porous, and the average pore diameter was <1 μm. On the other hand, the cross section of PS15 fiber cured by electron beam irradiation is not porous. However, the fiber

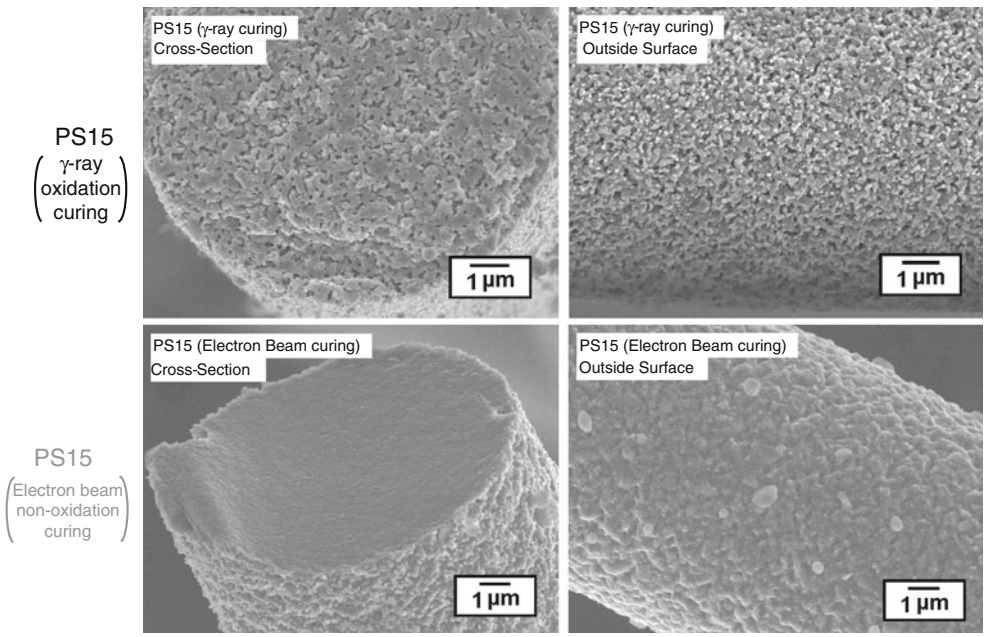

Fig. 9 The FE-SEM images of PS15 fibers re-pyrolyzed at 1773 K in 0.5 h

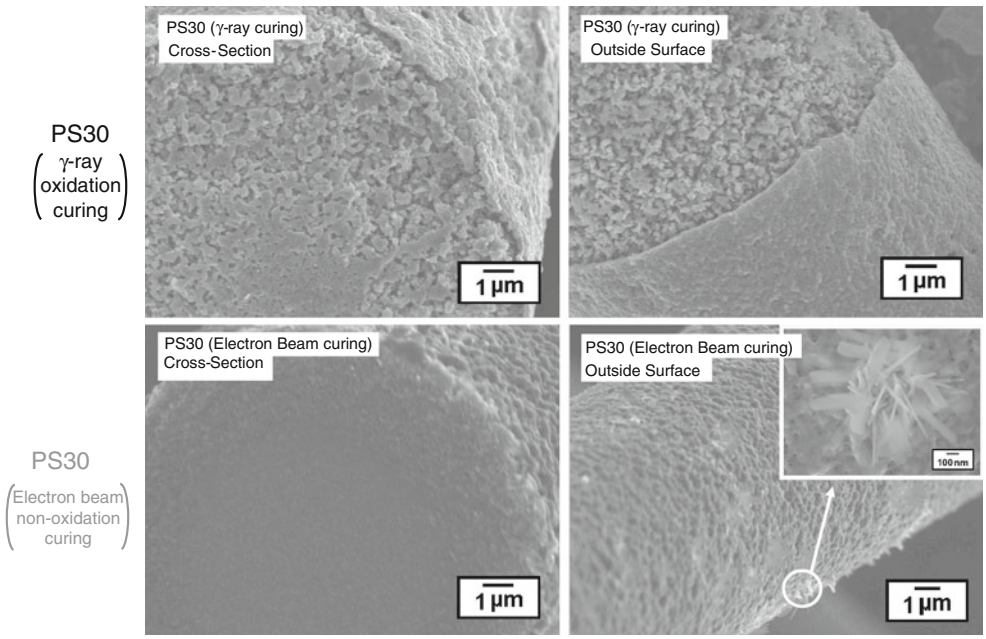

Fig. 10 The FE-SEM images of PS30 fibers re-pyrolyzed at 1773 K in 0.5 h

surface is covered by crystallized grains. Figure 10 shows the FE-SEM images of PS30 fibers re-pyrolized at 1773 K for 0.5 h in an inert atmosphere. The cross section of PS30 fibers cured by γ-ray oxidation was porous. The pores in the cross section were not uniformly distributed. Near the center of the fiber, the structure was relatively dense. In the vicinity of the fiber surface, however, number of the pores was increased. On the other hand, there were no pores in the cross section of PS30 fibers cured by electron beam irradiation. On the outside surface of the fiber, there were a number of needle-like crystals.

As shown in Figs. 9 and 10, the PS15 and PS30 fibers which were cured by γ-ray oxidation and re-pyrolyzed at 1773 K became porous ceramic fibers. In order to estimate the existence of fine pores, the surface area of these fibers was measured. Figure 11 shows the surface areas of PCS, PS15, and PS30 fibers after re-pyrolysis at 1573–1773 K. The surface area of re-pyrolyzed PCS increased at 1673 and 1723 K, and the maximum was approximately 4 m^2/g. In the case of PS15 and PS30 fibers, surface areas started to increase at 1573 K and kept increasing up to 1673 K, after which they turned to decrease at 1773 K. The maximum surface areas for PS15 and PS30 fibers, respectively, were 102 and 152 m^2/g. At high temperatures beyond 1573 K, microstructural changes in the fiber are known to proceed

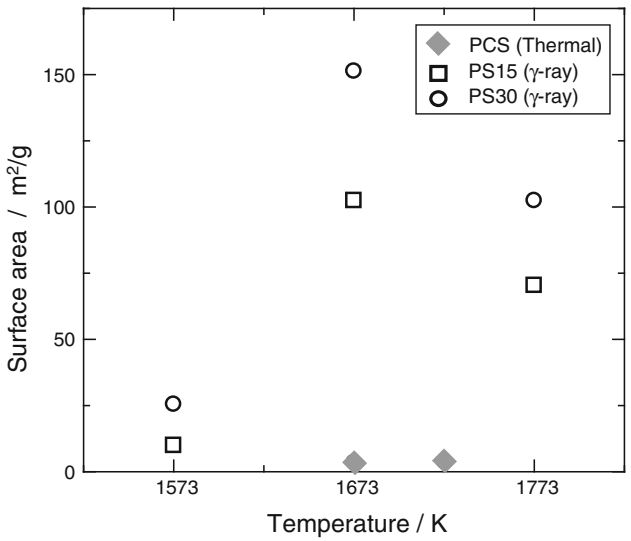

Fig. 11 The surface areas of PCS, PS15, and PS30 fibers after re-pyrolysis at 1773 K under inert atmosphere

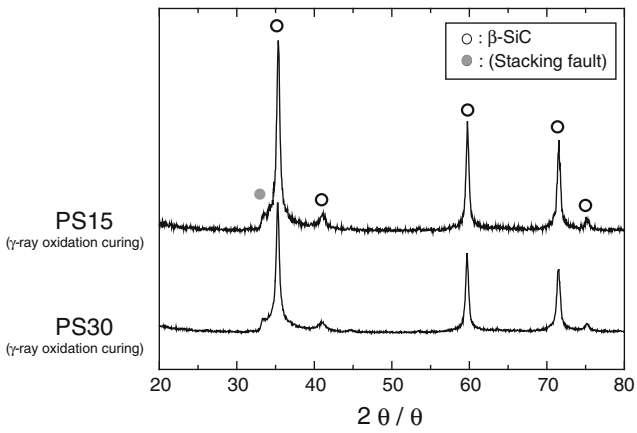

Fig. 12 The X-ray diffraction patterns (CuKa) of PS15 and PS30 fibers after re-pyrolysis at 1773 K under inert atmosphere

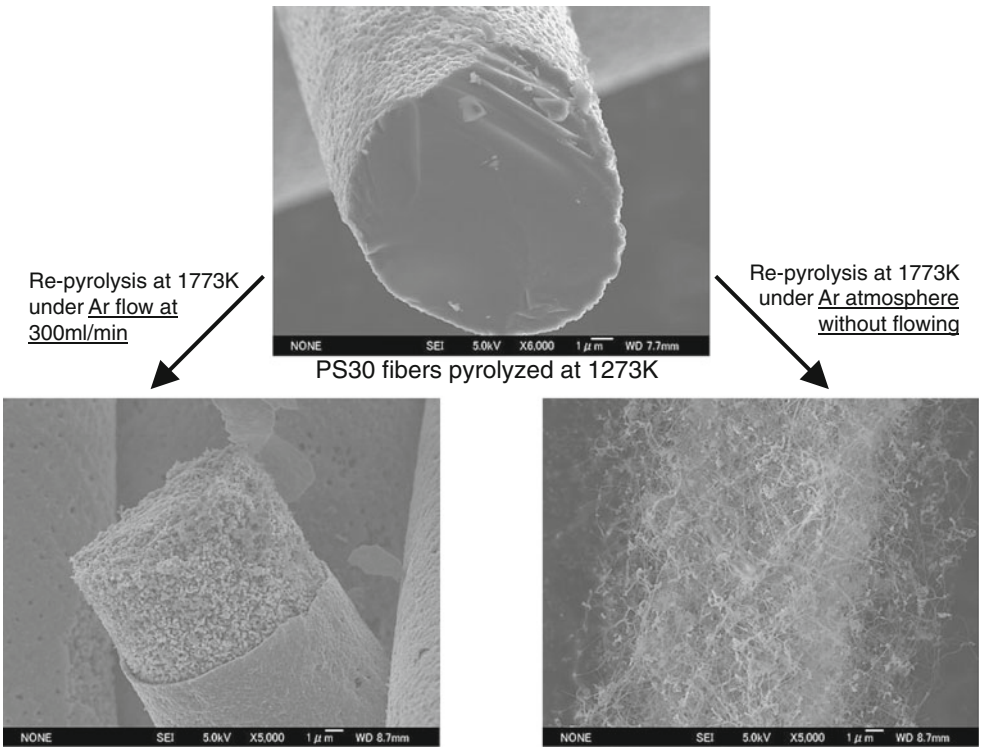

Fig. 13 The FE-SEM images of PS30 fibers after re-pyrolysis at 1773 K under inert atmosphere

with the evolution of CO and SiO. The PS fiber with γ-ray curing showed high mass loss relative to the PCS fiber. Based on the observed porous structure, gas evolution and microstructural changes proceed not only at the fiber surface, but also at inner areas of the fiber. High numbers of Si–O bonds from siloxane chains and free carbons from phenyl groups are thought to drive rapid and large microstructural changes at many nucleation sites distributed in the fiber. SiC nanocrystal formation, evolution of a basic structural unit of carbon, and inhibition of SiC crystal aggregation with free carbon at the grain boundary, may contribute to the high surface areas observed. SiC crystal growth in PS fibers was confirmed by XRD (Fig. 12).

Figure 13 shows SEM images of PS30 fibers re-pyrolyzed at 1773 K. One shows a porous ceramic fiber obtained after re-pyrolysis under Ar flow (300 mL/min). The other shows a fiber re-pyrolyzed under Ar flow at 5 mL/min. The fiber surface is densely covered with SiC nanowires, which may be formed by a vapor phase reaction ($SiO + 3CO > SiC + 2CO_2$). Such nanowire formation may be effective in further increasing the specific surface area by controlling the fiber pyrolysis atmosphere [15].

Conclusion

PMPhS exhibited a strong plasticizer effect on PCS with high compatibility up to 30 mass%. Despite the resulting thin diameters with improved melt-spinnability, the tensile strength after pyrolysis did not exceed that of the fibers derived from pure PCS. Bleed out of the PMPhS component during fiber pyrolysis could possibly be the cause of surface defects. Under high-temperature pyrolysis, the fiber structure became porous and large specific surface areas were obtained. These effects are considered to result from the reaction between Si–O bonds in the starting siloxane chains and free carbon from the starting phenyl groups. When gas flow rate was reduced, a SiC nanowire layer was formed on the fiber surface, presumably by vapor phase reactions involving CO and SiO. This constitutes further evidence of increased gas evolution and chemical reactions in PS fibers during high-temperature re-pyrolysis.

Acknowledgement This work is partly supported by a Grant-in Aid for Scientific Research C from Japan Society of Promotion Science.

References

1. Okamura K, Seguchi T (1992) J Inorg Organomet Polym 2:171
2. Ichikawa H (2006) J Ceram Soc Jpn 114:455
3. Yajima S, Hayashi J, Omori M, Okamura K (1976) Nature 261:683
4. Takeda M, Imai Y, Ishikawa T, Seguchi T, Okamura K (1991) Ceram Eng Sci Proc 12:1007
5. Kumagawa K, Yamaoka H, Shibuya M, Yamamura T (1997) Ceram Eng Sci Proc 18:987
6. Idesaki A, Narisawa M, Okamura K, Sugimoto M, Tanaka S, Morita Y, Seguchi T, Itoh M (2001) J Mater Sci 36:5565. doi: 10.1023/A:1012549228826

7. Narisawa M, Shimoda K, Nishioka M, Iseki T, Mabuchi H, Okamura K, Oka K, Dohmaru T (2006) J Ceram Soc Jpn 114:511
8. Harkness BR, Tachikawa M, Mita I (1995) Macromolecules 28:1323
9. Harkness BR, Tachikawa M, Mita I (1995) Macromolecules 28:8136
10. Ohta Y (2004) Sen'i Gakkaishi 60:270
11. Sugimoto M, Idesaki A, Tanaka S, Okamura K (2003) Key Eng Mater 247:133
12. Idesaki A, Narisawa M, Okamura K, Sugimoto M, Morita Y, Seguchi T, Itoh M (2001) Rad Phys Chem 60:483
13. Hasegawa Y, Okamura K (1983) J Mater Sci 18:3633. doi: 10.1007/BF00540736
14. Caberry E, West R (1966) J Organomet Chem 6:582
15. Bouillon E, Mocare D, Villenuve F, Pailler R, Naslain R, Monthioux M, Oberlin A, Guimon C, Pfister G (1991) J Mater Sci 26:1517. doi:10.1007/BF00544661